Published in final edited form as:
*Clin Cancer Res*. 2008 June 15; 14(12): 3993–4001. doi:10.1158/1078-0432.CCR-07-4152.

# PTEN Loss Does Not Predict for Response to RAD001 (Everolimus) in a Glioblastoma Orthotopic Xenograft Test Panel

**Lin Yang**[1], **Michelle J. Clarke**[2], **Brett L. Carlson**[1], **Ann C. Mladek**[1], **Mark A. Schroeder**[1], **Paul Decker**[6], **Wenting Wu**[6], **Gaspar J. Kitange**[1], **Patrick T. Grogan**[1], **Jennie M. Goble**[3], **Joon Uhm**[3], **Evanthia Galanis**[4], **Caterina Giannini**[5], **Heidi A. Lane**[7], **C. David James**[8], and **Jann N. Sarkaria**[1]

[1]Department of Radiation Oncology, Mayo Clinic, Rochester, Minnesota [2]Department of Neurosurgery, Mayo Clinic, Rochester, Minnesota [3]Department of Neurology, Mayo Clinic, Rochester, Minnesota [4]Department of Oncology, Mayo Clinic, Rochester, Minnesota [5]Laboratory Medicine and Pathology, Mayo Clinic, Rochester, Minnesota [6]Division of Biostatistics, Mayo Clinic, Rochester, Minnesota [7]Novartis Institute for BioMedical Research, Basel, Switzerland [8]Department of Neurological Surgery and Brain Tumor Research Center, University of California-San Francisco, San Francisco, California

## Abstract

**Purpose—**Hyperactivation of the phosphatidylinositol 3-kinase/Akt signaling through disruption of PTEN function is common in glioblastoma multiforme, and these genetic changes are predicted to enhance sensitivity to mammalian target of rapamycin (mTOR) inhibitors such as RAD001 (everolimus).

**Experimental Design—**To test whether PTEN loss could be used as a predictive marker for mTOR inhibitor sensitivity, the response of 17 serially transplantable glioblastoma multiforme xenografts was evaluated in an orthotopic therapy evaluation model. Of these 17 xenograft lines, 7 have either genomic deletion or mutation of PTEN.

**Results—**Consistent with activation of Akt signaling, there was a good correlation between loss of PTEN function and elevated levels of Akt phosphorylation. However, of the 7 lines with disrupted PTEN function, only 1 tumor line (GBM10) was significantly sensitive to RAD001 therapy (25% prolongation in median survival), whereas1 of 10 xenograft lines with wild-type PTEN was significantly sensitive to RAD001 (GS22; 34% prolongation in survival). Relative to placebo, 5 days of RAD001 treatment was associated with a marked 66% reduction in the MIB1 proliferation index in the sensitive GBM10 line (deleted PTEN) compared with a 25% and 7% reduction in MIB1 labeling index in the insensitive GBM14 (mutant PTEN) and GBM15 (wild-type PTEN) lines, respectively. Consistent with a cytostatic antitumor effect, bioluminescent imaging of luciferase-transduced intracranial GBM10 xenografts showed slowed tumor growth without significant tumor regression during RAD001 therapy.

**Conclusion—**These data suggest that loss of PTEN function is insufficient to adequately predict responsiveness to mTOR inhibitors in glioblastoma multiforme.



Requests for reprints: Jann N. Sarkaria, 200 First Street, SW, Rochester, MN 55905. Phone: 507-266-3877; Fax: 502-284-3906; sarkaria.jann@mayo.edu.

**Note:** Supplementary data for this article are available at Clinical Cancer Research Online (http://clincancerres.aacrjournals.org/).

**Disclosure of Potential Conflicts of Interest**

J. Sarkaria receives research funding from Novartis. H. Lane was an employee of Novartis when these studies were performed.

The mammalian target of rapamycin (mTOR) is an important modulator of mitogenic signaling in both normal and tumor cells, and small-molecule inhibitors of mTOR have shown promising activity in several tumor types (1–3). mTOR functions to integrate mitogenic signals with the nutrient status of the cell to promote cell growth and proliferation only under adequate nutrient conditions. mTOR signals to multiple components of the protein translation machinery to promote the translation of a subset of mRNA transcripts with complex 5′-untranslated regions (reviewed in ref. 4). Many of these gene products are important for driving tumor cell growth, proliferation, and angiogenesis, and the antitumor effects of mTOR inhibitors are predominantly linked to disruption of these processes.

Mitogenic activation of mTOR signaling is controlled in part through the phosphatidylinositol 3-kinase (PI3K)/Akt signaling pathway. Akt-mediated phosphorylation of both mTOR itself and the mTOR inhibitory molecule TSC2 can promote activation of mTOR signaling (5–8). The PI3K/Akt signaling pathway is commonly hyperactivated in glioblastoma multiforme through functional loss of the PTEN tumor suppressor protein. In keeping with the hypothesis that constitutive hyperactivity within a signaling pathway results in hypersensitivity to pathway inhibition, several studies in isogenic tumor models have shown that loss of PTEN function results in increased sensitivity to mTOR inhibitors (9–11). These observations have prompted several groups to propose clinical trials in which only those patients with tumors lacking PTEN function would be treated with a mTOR inhibitor-based regimen. However, other factors, such as energy deprivation and amino acid starvation, are also important mediators of mTOR activity (12–20), and given these data, it is not clear whether PTEN status is a major factor that influences *in vivo* responses to mTOR inhibitors in patient tumors.

We have reported previously the development of a panel of glioblastoma multiforme xenografts established from patient samples and passaged serially in the flank of nude mice, and we have used this panel for assessing the influence of epidermal growth factor receptor (EGFR) amplification status and PTEN status on responsiveness to the EGFR inhibitor erlotinib (21). To understand more fully whether PTEN status would be a useful predictor of response to therapy with the mTOR inhibitor RAD001 (everolimus), we correlated the molecular status of PTEN within our xenograft lines with the extent of survival prolongation for orthotopic tumors established from these lines following therapy with RAD001. The results of this study suggest that loss of PTEN function is insufficient to predict RAD001 sensitivity.

## Materials and Methods

### Cell culture assays

Established gliomas cell lines differing in PTEN status (PTEN−/−: LN401, BS125II.2, BS153, and U87; PTEN+/+: LN229, LN427, LN751, and LN428) were plated into 96-well plates, incubated overnight, and then treated with graded concentrations of RAD001. After 4 days of incubation at 37°C, cells were fixed onto the plates with 6% glutaraldehyde. After washing in water, cells were stained with methylene blue, washed, and incubated with 3% hydrochloric acid and absorbance was measured at 650 nm. The $IC_{50}$ values (RAD001 concentration that reduces methylene blue staining by 50%) for each line were calculated using Softmax 1.2.0 software. U87 and U251 cells also plated and treated with RAD001 as described above and then pulsed with [$^3$H]thymidine for 2 h. Cells were harvested by trypsinization, transferred onto glass filters, and lysed in distilled water. Filter-bound radioactivity was determined by liquid scintillation counting.

### Xenograft information

Each of the 17 serially passaged xenografts used in this study were derived from tumors of different patients. Molecular genetic alterations and corresponding patient tumor histopathologic classifications for 15 of xenografts have been described previously (21, 22): 2 additional xenografts not reported previously, GBM16 and GBM34, both diagnosed as glioblastoma, have been included in the current investigation. Prior institutional review board authorization was obtained for the use of human tissue to establish the xenograft lines.

### Orthotopic xenograft model and therapy response experiments

All xenograft therapy evaluations were conducted using an orthotopic tumor model and a protocol approved by the Mayo Institutional Animal Care and Use Committee. Flank tumor xenografts were harvested, mechanically disaggregated, and grown in short-term cell culture (5–14 days) in DMEM supplemented with fetal bovine serum, 1% penicillin, and 1% streptomycin. Cells were harvested by trypsinization and injected with $3 \times 10^5$ cells into the right basal ganglia of anesthetized athymic nude mice (Ncr-*nu/nu*, National Cancer Institute). Before treatment initiation, animals were randomized to treatment and control groups of 5 to 10 mice each. RAD001 therapy was initiated 2 weeks before the time mice were expected to become moribund. A microemulsion of RAD001 (10 mg/kg/d, Monday–Friday) or the corresponding vehicle control (courtesy of Dr. Heidi Lane, Novartis Institutes for BioMedical Research, Oncology Basel) was administered by oral gavage until mice became moribund or a minimum of 4 weeks of treatment was completed. All mice used for therapy response evaluations were observed daily and euthanized at the time of reaching a moribund condition.

### Bioluminescence imaging

GBM10 xenograft cells were transduced with an HIV1-based lentiviral vector expressing firefly luciferase (Fluc) as described previously (21). Fluc-modified GBM10 cells were used to establish intracranial tumors that were monitored for RAD001 response by longitudinal bioluminescence imaging. For bioluminescent imaging, mice were injected with 100 μg luciferin, simultaneously anesthetized with ketamine/xylazine, and subsequently imaged with a cooled CCD camera (IVIS 200; Xenogen). Tumor light output was quantitated using the Living Image 2.5 software package (Xenogen). For each imaging session, relative light output for each mouse was normalized to the pretreatment value.

### Immunoblotting

Flank tumor tissues were lysed in a detergent-containing buffer: 50 mmol/L HEPES (pH 7.6), 30 mmol/L NaPPi, 10 mmol/L NaF, 150 mmol/L NaCl, 1 mmol/L EDTA, 1% Triton X-100, 10 ng/mL aprotinin, 10 ng/mL pepstatin, 10 ng/mL leupeptin, 20 nmol/L microcystin, 0.1 mmol/L phenylmethylsulfonyl fluoride, and 1 mmol/L sodium orthovanadate. Lysates were cleared of insoluble material by centrifugation. Samples were boiled in SDS sample buffer, equal amounts of protein were loaded and electrophoresed through SDS-PAGE gels, and resolved proteins were transferred to Immobilon-P membranes (Millipore). Membranes were blocked with 5% milk dissolved in TBS containing 0.02% Tween 20 and then incubated with primary antibody diluted in the same buffer. After washing, membranes were incubated with either goat anti-rabbit (Cell Signaling) or goat anti-mouse (Pierce) antibodies conjugated to horseradish peroxidase. Blots were developed with Super Signal Chemiluminescence reagent (Pierce). Immunoblotting was done with phosphospecific antibodies first and then membranes were stripped and reprobed with the relevant antibodies against corresponding total protein. Antibodies used in this study for detection of total mTOR, phospho-S2481 mTOR, total p70S6 kinase, phospho-T389 p70S6 kinase, total S6, phospho-S240/244 S6, EGFR, total

PTEN, total Erk, phospho-T202/Y204 Erk, total Akt, phospho-T308 Akt, phospho-S473 Akt, total STAT3, phospho-Y705 STAT3, total GSKβ, phospho-S9 GSKβ, total TSC2, and phospho-T1462 TSC2 were all obtained from Cell Signaling; antibody for detection of β-actin was obtained from Sigma.

### Immunohistochemistry

Brains from mice with intracranial tumor were resected and then bisected along the needle tract used for injecting the tumor cells. Half of each bisected brain was placed in formalin and subsequently embedded in paraffin. The other half of each brain was frozen in OCT. MIB1 immunohistochemistry and quantitation of MIB1 labeling index were done as described previously (21). For CD31 analysis, frozen sections of corresponding OCT-embedded tissues were fixed in acetone and stained with rat anti-mouse CD31α antibody (clone MEC13.3; BD PharMingen) at a 1:50 dilution. The number of CD31-staining microvessels for each tumor section was quantified in three fields at ×60 magnification. Terminal deoxynucleotidyl transferase–mediated dUTP nick end labeling analysis was done using the ApopTag Plus Peroxidase *In Situ* apoptosis detection kit (Chemicon) as described previously (21).

For phospho-S6 IHC, paraffin-embedded sections were deparaffinized with HistoClear and rehydrated with ethanol washes. Following steam citrate antigen retrieval, slides were incubated with a rabbit polyclonal anti-phospho-S240/244 S6 antibody (Cell Signaling Technologies). After incubation with a goat anti-rabbit secondary antibody and ABC reagent (Vector Laboratories), staining was developed with NovaRed Developing Reagent, and slides were counterstained with hematoxylin.

### Reverse transcription-PCR

Tumor tissue was homogenized in TRIzol (Invitrogen) and subsequently clarified by centrifugation. Chloroform/isopropanol extraction was used to isolate RNA, and cDNA was synthesized with an oligo(dT) primer and MMLV reverse transcriptase (Promega). PCR amplification of human PTEN transcripts was done using PCR primers that specifically recognize human, but not murine, PTEN (23). PCR for β-actin was done as a control as described (24).

### Statistics

Comparison of $IC_{50}$ values for PTEN−/− and PTEN+/+ tumor cells was done using a rank-sum test. Cumulative survival probabilities were estimated using the Kaplan-Meier method. Survival of treatment groups was compared using the log-rank test. Survival was also compared between groups using the $\chi^2$ test. For this analysis, the median survival was calculated for both groups combined (placebo + RAD001). Following this, mice in each group were classified as living greater than or less than the median survival. The $\chi^2$ test was then used to compare the two groups on the percentage of mice that lived longer than the combined median survival. A *t* test was used to compare proliferation rates, apoptosis, and CD31 microvessel density in control-and RAD001-treated groups. A repeated-measures ANOVA with an autoregressive correlation structure was used to compare luminescent imaging between the RAD001 and placebo groups. For this analysis, tumor luminescence value was the dependent variable and treatment group was the independent variable. In call cases, $P$ values ≤ 0.05 were considered statistically significant.

## Results

### Comparison of *in vitro* evaluation of RAD001 response

The sensitivity of four established glioblastoma multiforme xenograft lines with wild-type PTEN status (+/+) and four glioblastoma multiforme lines lacking PTEN function (−/−) was evaluated in an *in vitro* cell growth assay, and the concentration associated with 50% inhibition of growth ($IC_{50}$) was calculated for each line. As seen in Fig. 1A, cell lines lacking wild-type PTEN function were significantly more sensitive to RAD001 (median $IC_{50}$, 3.5 nmol/L) compared with cell lines with wild-type PTEN function (median $IC_{50}$, 22.9 nmol/L; $P = 0.03$). In a parallel study, the RAD001 sensitivity of U87 and U251 glioma lines, which both lack PTEN function, were tested both *in vitro* and *in vivo*. Following a 96-hour incubation with RAD001, cellular proliferation, as measured by [$^3$H]thymidine uptake, was reduced to a significantly greater extent in U87 cells ($^3$H uptake was 43% of control at 10 nmol/L; Fig. 1B) compared with U251 ($^3$H uptake was 83% of control at 10 nmol/L; $P = 0.01$). In contrast, orthotopic U87 xenografts were resistant to daily oral systemic therapy with RAD001 (median survival, 39 versus 38 days for placebo versus RAD001 treatment; $P = 0.92$, log-rank), whereas treatment of orthotopic U251 xenografts with RAD001 significantly prolonged survival (median survival, 32 versus 52 days for placebo versus RAD001 treatment; $P = 0.007$, log-rank; Fig. 1C and D). A similar pattern of mTOR inhibitor sensitivity was seen in flank tumor regrowth delay assays in which mTOR inhibition by rapamycin was significantly more effective at suppressing tumor growth in U251 xenografts compared with U87 xenografts (data not shown; ref. 25). Because of the significant discrepancy between *in vitro* and *in vivo* results, we elected to test RAD001 in an orthotopic therapy evaluation model using our unique panel of 17 xenograft lines.

### PTEN status in the Mayo glioblastoma multiforme xenograft panel

Given the potential importance of PTEN function in modulating mTOR inhibitor sensitivity, the molecular and genetic status of PTEN was assessed in the Mayo glioblastoma multiforme xenograft panel using four independent methods: direct genomic sequencing, genomic PCR, human-specific reverse transcription-PCR, and Western blotting. The former two assays showed intact wild-type genomic PTEN genes in 9 of 17 xenograft lines, PTEN sequence mutations in 2 of 17 lines, and homozygous deletion of PTEN in 5 of 17 lines (Table 1). Consistent with this genomic analysis, no PTEN mRNA was detected by reverse transcription-PCR in the xenograft lines found to have homozygous deletion of PTEN, whereas PTEN mRNA was detected in tumor lines with either wild-type or mutant PTEN coding sequence (Fig. 2A). However, significant accumulation of PTEN protein was observed only in xenografts with wild-type PTEN sequence and in GS28 with a PTEN point mutation (Fig. 2B). Consistent with hyperactivation of PI3K signaling, lack of PTEN expression was associated with increased phosphorylation of Akt on both S473 and T308 (Fig. 2C; data not shown). A weaker correlation was observed between Akt phosphorylation and phosphorylation of its downstream targets GSK3β on Ser[9] and TSC2 on T1462. Thus, within this genetically diverse panel of tumors, there is a broad range in the level of PI3K/Akt signaling associated with loss of PTEN function.

### Survival analysis with RAD001 treatment

Sensitivity of each xenograft line to RAD001 was determined in a series of survival experiments. Groups of mice with established intracranial xenografts, derived from each of the 17 glioblastoma multiforme xenograft lines, were randomized and treated with RAD001 or placebo. Therapy was initiated ~2 weeks before the mice developing signs of advanced

[9] http://dtp.nci.nih.gov/dtpstandard/InvivoSummary/index.jsp

tumor burden in an effort to mimic the likely use of this agent in patients with clinically evident tumor. In several tumor lines, the survival experiments were repeated one or more times to confirm the benefit or lack of benefit for RAD001 therapy. The results from all experiments for a given tumor line were pooled for analysis and are presented in Table 1. The corresponding survival curves for each xenograft line can be found in Supplementary Fig. S1. Two statistical methods were used to determine survival benefit: log-rank test and a $\chi^2$ test as described in the statistical methods. From these analyses, two xenograft lines, GBM10 and GS22, were identified as being significantly sensitive to RAD001 therapy by both tests (Fig. 3A and B). RAD001 treatment resulted in 25% prolongation in median survival for GBM10 (PTEN deleted; $P < 0.001$, log-rank and $P < 0.001$, $\chi^2$) and 34% prolongation in median survival for GS22 (PTEN wild-type; $P = 0.002$, log-rank and $P = 0.005$, $\chi^2$). In two other xenograft lines, RAD001 treatment was associated with a marginal but significant prolongation in survival by one but not both statistical assays (Fig. 3C and D): 12% survival prolongation in GS28 (PTEN mutant; $P = 0.04$, log-rank, $P = 0.13$, $\chi^2$) and 11% survival prolongation in GBM44 (PTEN wild-type; $P = 0.75$, log-rank, $P = 0.05$, $\chi^2$). In light of the limited survival benefit observed in these two lines, we conclude that only GBM10 and GBM22 are robustly sensitive to RAD001 therapy.

## Activation status of EGFR and mTOR signaling pathways

Presumably, tumor lines with constitutive activation of mTOR signaling should be more sensitive to mTOR inhibition. Therefore, autophosphorylation of mTOR at S2481 was evaluated. Interestingly, mTOR phosphorylation was quite low in the sensitive GBM10 xenograft (PTEN deleted) and relatively elevated in the sensitive GBM22 line (PTEN wild-type; Fig. 4). Downstream from mTOR, there was a poor correlation between mTOR activation and phosphorylation levels within the activation loop (T389) of p70S6K or the downstream p70S6K target, ribosomal S6 protein, and there was no apparent correlation with phosphorylation of these targets and sensitivity to RAD001 (Fig. 4).

EGFR amplification occurs in ~40% of primary glioblastoma multiforme tumors, which can contribute to constitutive activation of the PI3K and mitogen-activated protein kinase signaling pathways. Similar to the incidence in primary tumors, high-level EGFR amplification (22, 26) and expression (Supplementary Fig. S2) were observed in 7 of 17 (41%) xenograft lines. High-level EGFR expression was associated with elevated Erk phosphorylation, although several lines lacking EGFR expression also maintained significant levels of Erk phosphorylation (Supplementary Fig. S2). Similarly, with the exception of GBM6, EGFR overexpression was associated with increased STAT3 phosphorylation, although several lines with low EGFR expression also had elevated phospho-STAT3 (Supplementary Fig. S2). As in the mTOR signaling analysis, there was no apparent correlation between EGFR amplification and mTOR sensitivity, although both RAD001-sensitive tumor lines lacked EGFR amplification or evidence of constitutive EGFR signaling.

## RAD001 effects on proliferation, apoptosis, and angiogenesis

The antitumor effects of mTOR inhibitors have been variably attributed to inhibition of tumor proliferation, induction of apoptosis, and/or inhibition of angiogenesis. To assess the influence of RAD001 on these processes in both sensitive and resistant xenograft lines, mice with established intracranial tumors derived from GBM10, GBM14, and GBM15 were randomized to treatment with placebo or RAD001 for 5 days and then mice were euthanized and tumors were sectioned for analysis. RAD001 treatment resulted in a marked reduction in tumor proliferation in GBM10 (Fig. 5A; 44 ± 8% labeling index with placebo versus 17 ± 6% with RAD001; $P < 0.001$), a modest reduction in proliferation in GBM14 (40 ± 8% versus 32 ± 11%, respectively; $P = 0.03$), and no effect on proliferation in GBM15 (57 ± 6%

versus 53 ± 6%, respectively; $P = 0.46$). Consistent with efficient inhibition of mTOR signaling in the resistant GBM15 tumor, S6 phosphorylation levels were significantly suppressed in intracranial tumor sections derived from mice treated with RAD001 (Fig. 5B).

mTOR inhibitors are associated with inhibition of angiogenesis and induction of apoptosis; therefore, we also evaluated the effects of RAD001 on these two processes using the same treated and untreated tumor samples described above. In contrast to the effects on proliferation, RAD001 had no significant effect on the induction of apoptosis in any of the three lines, with the fraction of terminal deoxynucleotidyl transferase–mediated dUTP nick end labeling–positive cells being <3% in all tumor lines regardless of treatment (Supplementary Fig. S3A). Similarly, RAD001 treatment had no significant effect on CD31 microvessel density or vascular endothelial growth factor expression levels. The density of $CD31^+$ microvessels following 5 days of treatment with placebo or RAD001 were 10 ± 4 versus 12 ± 6 vessels/high-power field, respectively, for GBM10 ($P = 0.6$), 26 ± 6 versus 24 ± 6 vessels/high-power field, respectively, for GBM14 ($P = 0.5$) and 17 ± 7 versus 19 ± 7 vessels/high-power field, respectively, for GBM15 ($P = 0.6$; Supplementary Fig. S3B). Thus, the efficacy of RAD001 in our xenograft model system does not appear related to either induction of apoptosis or suppression of angiogenesis.

To follow-up these mechanistic studies, the influence of RAD001 on intracranial tumor burden was monitored over time using bioluminescent imaging. GBM10 cells were infected with a lentivirus containing a firefly luciferase expression cassette, and the Fluc-expressing cells were used to establish orthotopic xenografts. Once all mice had detectable luciferase activity by bioluminescent imaging, then mice were randomized and treated with placebo or RAD001 starting on day 20. As seen in Fig. 5C and D, RAD001 treatment was associated with a significantly lower level of tumor luminescence, and once RAD001 treatment was discontinued, the luminescence output from the tumors markedly accelerated. In a repeated-measures ANOVA model fit over four observations [days 16 (before drug treatment), 24, 31, and 38] RAD001 had significant lower levels of tumor luminescence compared with placebo treated mice ($P = 0.01$). After the day 38 observation point, all placebo mice were dead. Collectively, the immunohistochemical analyses and the bioluminescent study are consistent with a predominantly cytostatic mechanism of antitumor effect by RAD001.

## Discussion

The goal of molecular oncology is to identify the most efficacious therapy for an individual patient based on their tumor molecular phenotype. Previous studies have suggested that activation of the PI3K/Akt/mTOR signaling pathway resulting from loss of PTEN function would predict for sensitivity to mTOR inhibitor therapy, and in this study, we tested this hypothesis in an intracranial therapy evaluation model using a panel of glioblastoma multiforme xenografts. In contrast to traditional cultured cell lines in which EGFR amplification and normal PTEN function are often lost, our method for establishing and maintaining human glioblastoma multiforme xenografts by serial transplantation in the flank of nude mice allows for preservation of EGFR amplification status (26) and maintenance of PTEN expression. To maximize the clinical relevance of these studies, response to therapy was studied in an orthotopic model with chronic RAD001 dosing initiated in mice with established intracranial tumors. Using this model, we identified 2 of the 17 xenograft lines (12%) in which chronic RAD001 dosing significantly extended survival of tumor-bearing mice (GBM10 and GS22). However, in contrast to expectations, PI3K/Akt activation associated with loss of PTEN function was observed in only 1 of 2 sensitive xenografts (GBM10). These data suggest that PTEN expression or Akt activation status may not be a sufficiently robust predictor of mTOR inhibitor responsiveness in glioblastoma multiforme to allow assignment of therapy.

Two clinical studies have evaluated monotherapy with a mTOR inhibitor (CCI-779/temsirolimus) in patients with recurrent glioblastoma multiforme, and the extent of benefit in these studies is similar to that seen in our xenograft panel. In a North Central Cancer Treatment Group study of 68 patients with recurrent glioblastoma multiforme, no patients met the criteria for an objective response (>25% tumor shrinkage), although 36% of patients had improvement in the extent of T2 signal abnormality on magnetic resonance imaging, and these "responding" patients had a significantly longer median time to progression (5.4 months) compared with "nonresponders" (1.9 months; ref. 27). Interestingly, in this study, there was no correlation between PTEN deletion or lack of expression and these imaging responses. In a similar study by the North American Brain Tumor Consortium, 43 patients with recurrent glioblastoma multiforme were treated with CCI-779. Two patients had partial responses and 20 patients were classified as having stable disease, although the median time to progression was only 2.1 months (28). Similar to these clinical results (objective tumor shrinkage observed in only 2 of 111 patients treated on these two clinical trials), RAD001 treatment in the sensitive GBM10 xenograft line was associated with inhibition of tumor growth, as measured by bioluminescent imaging, without significant tumor regression (Fig. 5D). Consistent with a predominantly cytostatic mechanism of action, RAD001 treatment resulted in a 61% reduction in proliferative rate in GBM10 (Fig. 5A) but had no effect on apoptosis induction (Supplementary Fig. S3A). In contrast to a previous study with GL261 heterotopic glioma xenografts (29), RAD001 did not have an appreciable affect on microvessel density. Although the antiangiogenic effects of RAD001 and other mTOR inhibitors are well established in nonglioma tumor models (30–32), the lack of effect of RAD001 on microvessel density suggest that suppression of angiogenic signaling is not required for the cytostatic effects of RAD001.

The limited numbers of clinical responses to mTOR inhibitor therapy in recurrent glioblastoma multiforme and the relatively low frequency of sensitive tumors in our xenograft panel are in distinct contrast to our *in vitro* studies using established glioblastoma multiforme tumor lines (Fig. 1A) and previously published studies in traditional glioma models. Prolongation in survival with mTOR inhibitor therapy has been published in U251 and D54 orthotopic glioma xenografts and in U87, U251, D54, and GL261 heterotopic xenografts[9] (29, 33–36). Orthotopic U87 xenografts are the only tumor line that has been reported previously as being resistant to mTOR inhibitor therapy (35). This high rate of sensitivity to mTOR inhibitors in xenografts derived from conventional cell lines partly may reflect adaptive changes associated with the long-term culturing of tumor cells *in vitro*. Location of tumor implantation likely is an important determinant of responsiveness. In one study, suppression of tumor growth by rapamycin in U87 flank tumors was associated with inhibition of vascular endothelial growth factor expression, whereas U87 orthotopic tumors had much lower vascular endothelial growth factor expression and were insensitive to RAD001 therapy (35). These results highlight the potential influence of tumor microenvironment on responsiveness to molecular inhibitors. Consistent with this idea, we and others have observed that relative sensitivities of U87 and U251 are significantly different *in vitro* versus *in vivo* (Fig. 1; ref. 36), although we have not observed differences in sensitivity to mTOR inhibition in these two lines when grown in the orthotopic versus heterotopic position. Presumably, the discrepancy between *in vitro* and *in vivo* responsiveness to RAD001 reflects the central role mTOR plays in modulating tumor cell growth and proliferation in response to nutrient and energy stressors that are not normally encountered in cell culture conditions. Drug penetration through the blood-brain barrier also is an important determinant of drug efficacy in brain tumors. Although we have not formally tested the integrity of the blood-brain barrier of orthotopic xenografts derived from our xenograft lines, RAD001 was effective at inhibiting mTOR signaling to ribosomal S6 protein in at least one RAD001-resistant xenograft line grown in an orthotopic position (GBM15; Fig. 5B). Thus, the selection of tumor models and growth conditions can have

significant influence on the clinical translatability of laboratory studies directed at identifying relevant clinical markers for mTOR inhibitor sensitivity in glioblastoma multiforme.

Hyperactivation of the PI3K/Akt/mTOR pathway through inactivation of PTEN has been linked to increased sensitivity to mTOR inhibitors in multiple tumor models and has been suggested as a potential molecular marker of mTOR inhibitor sensitivity (37). Similar to the incidence of PTEN loss in human tumor specimens, 7 of 17 xenografts tested had inactivation of PTEN function either through homozygous deletion or mutation. However, of the two RAD001-sensitive xenografts, only GBM10 is homozygous deleted with an associated lack of detectable PTEN transcript by reverse transcription-PCR (Fig. 2), whereas the other sensitive tumor, GS22, has wild-type PTEN sequence and detectable expression level by reverse transcription-PCR and Western blotting. PTEN protein expression was inversely associated with Akt phosphorylation levels in most, but not all, xenograft lines, which is similar to results from studies of clinical specimens (38, 39). Consistent with low-level Akt signaling activity in the RAD001-sensitive GS22, phosphorylation of the Akt substrate GSK-3β on S9 was significantly reduced relative to GBM10. Interestingly, auto-phosphorylation at S2481 of mTOR and phosphorylation of the downstream p70S6 kinase molecule was poorly correlated with Akt activation status, and neither marker correlated with responsiveness to RAD001 in GBM10 or GS22. This discrepancy between Akt and mTOR activation status is consistent with a recent analysis in which phosphorylation states of Akt and mTOR were poorly correlated in human glioblastoma multiforme patient tumor specimens assessed by immunohistochemistry (40). Both this latter study in patient tumor specimens and the current study in xenograft tissues suggest that Akt phosphorylation status or PTEN functional status likely will not be robust predictors of response to mTOR inhibitor therapies in clinical trials.

Presumably, this lack of correlation reflects the importance of other signaling pathways independent of PI3K/Akt that can modulate mTOR function. Specifically, TSC2 function is regulated not only by Akt but also by mitogen-activated protein kinase and AMP-activated protein kinase signaling pathways, and mTOR activity is affected directly by hypoxia and amino acid starvation. Recent studies have shown that p53 signaling through AMP-activated protein kinase can suppress mTOR function (41). Given that GS22 has mutated p53 (data not shown), one possibility is that loss of this p53/AMP-activated protein kinase inhibitory mechanism in GS22 allows for mTOR activation in the face of wild-type PTEN function and may be important for sensitivity to RAD001 *in vivo*. This hypothesis could be readily tested by restoring wild-type p53 expression in these cells and then evaluating the *in vivo* response to RAD001. This opportunity to generate alternative hypotheses regarding RAD001 sensitivity highlights the advantage of testing novel therapeutic agents in a genetically diverse panel of human glioblastoma multiforme xenografts.

In conclusion, through an evaluation of 17 xenograft lines, we have identified 2 glioblastoma multiforme xenografts that are significantly sensitive to the mTOR inhibitor RAD001. These results are consistent with clinical data and emphasize the value of *in vivo* testing in our xenograft panel for evaluating novel therapeutic strategies. In contrast to *in vitro* response data in established glioblastoma multiforme lines, there was a poor correlation between loss of PTEN function in our xenograft lines and RAD001 response *in vivo*. These results suggest that PTEN expression alone may be a poor predictor of mTOR inhibitor therapy response in patients.

## Supplementary Material

Refer to Web version on PubMed Central for supplementary material.

## Acknowledgments

**Grant support:** NIH grants NS49720 and CA097257 (C.D. James) and CA108961, CA25224, and CA114740 (J.N. Sarkaria, E. Galanis, and C. Giannini); American Cancer Society Research Scholar Grant (J.N. Sarkaria); and Accelerate Brain Cancer Cure (J.N. Sarkaria and C.D. James).

We thank Dr. Monika Hegi (Department of Neurosurgery, University Hospital Lausanne) and Dr. Adrian Merlo (Laboratory of Molecular Neuro-Oncology, University Hospital Basel) for providing the glioblastoma cell lines, Marc Hattenberger (Novartis Institutes for BioMedical Research, Oncology Basel) for performing the $IC_{50}$ determinations in the glioblastoma multiforme line panel, Cory Petell (Department of Oncology, Mayo Clinic) for transduction of cells with lentivirus, and James Tarara (Flow Cytometry and Optical Morphology Core, Mayo Clinic) for expert assistance in image analysis.

## References

1. Chan S, Scheulen ME, Johnston S, et al. Phase II study of temsirolimus (CCI-779), a novel inhibitor of mTOR, in heavily pretreated patients with locally advanced or metastatic breast cancer. J Clin Oncol. 2005; 23:5314–22. [PubMed: 15955899]
2. Hudes G, Carducci M, Tomczak P, et al. Temsirolimus, interferon α, or both for advanced renal-cell carcinoma. N Engl J Med. 2007; 356:2271–81. [PubMed: 17538086]
3. Witzig TE, Geyer SM, Ghobrial I, et al. Phase II trial of single-agent temsirolimus (CCI-779) for relapsed mantle cell lymphoma. J Clin Oncol. 2005; 23:5347–56. [PubMed: 15983389]
4. Rao RD, Buckner JC, Sarkaria JN. Mammalian target of rapamycin (mTOR) inhibitors as anti-cancer agents. Curr Cancer Drug Targets. 2004; 4:621–35. [PubMed: 15578919]
5. Sekulic A, Hudson CC, Homme JL, et al. A direct linkage between the phosphoinositide 3-kinase-AKT signaling pathway and the mammalian target of rapamycin in mitogen-stimulated and transformed cells. Cancer Res. 2000; 60:3504–13. [PubMed: 10910062]
6. Inoki K, Li Y, Zhu T, Wu J, Guan KL. TSC2 is phosphorylated and inhibited by Akt and suppresses mTOR signalling. Nat Cell Biol. 2002; 4:648–57. [PubMed: 12172553]
7. Manning BD, Tee AR, Logsdon MN, Blenis J, Cantley LC. Identification of the tuberous sclerosis complex-2 tumor suppressor gene product tuberin as a target of the phosphoinositide 3-kinase/akt pathway. Mol Cell. 2002; 10:151–62. [PubMed: 12150915]
8. Potter CJ, Pedraza LG, Xu T. Akt regulates growth by directly phosphorylating Tsc2. Nat Cell Biol. 2002; 4:658–65. [PubMed: 12172554]
9. Neshat MS, Mellinghoff IK, Tran C, et al. Enhanced sensitivity of PTEN-deficient tumors to inhibition of FRAP/mTOR. Proc Natl Acad Sci. 2001; 98:10314–9. [PubMed: 11504908]
10. Shi Y, Gera J, Hu L, et al. Enhanced sensitivity of multiple myeloma cells containing PTEN mutations to CCI-779. Cancer Res. 2002; 62:5027–34. [PubMed: 12208757]
11. Podsypanina K, Lee RT, Politis C, et al. An inhibitor of mTOR reduces neoplasia and normalizes p70/S6 kinase activity in Pten+/− mice. Proc Natl Acad Sci. 2001; 98:10320–5. [PubMed: 11504907]
12. Dennis PB, Jaeschke A, Saitoh M, Fowler B, Kozma SC, Thomas G. Mammalian TOR: a homeostatic ATP sensor. Science. 2001; 294:1102–5. [PubMed: 11691993]
13. Nave BT, Ouwens M, Withers DJ, Alessi DR, Shepherd PR. Mammalian target of rapamycin is a direct target for protein kinase B: identification of a convergence point for opposing effects of insulin and amino-acid deficiency on protein translation. Biochem J. 1999; 344:427–31. [PubMed: 10567225]
14. Hara K, Yonezawa K, Weng Q-P, Kozlowski MT, Belham C, Avruch J. Amino acid sufficiency and mTOR regulate p70 S6 kinase and eIF-4E BP1 through a common effector mechanism. J Biol Chem. 1998; 273:14484–94. [PubMed: 9603962]
15. Patel J, Wang X, Proud CG. Glucose exerts a permissive effect on the regulation of the initiation factor 4E binding protein 4E-BP1. Biochem J. 2001; 358:497–503. [PubMed: 11513750]
16. Arsham AM, Howell JJ, Simon MC. A novel hypoxia-inducible factor-independent hypoxic response regulating mammalian target of rapamycin and its targets. J Biol Chem. 2003; 278:29655–60. [PubMed: 12777372]

17. Long X, Ortiz-Vega S, Lin Y, Avruch J. Rheb binding to mammalian target of rapamycin (mTOR) is regulated by amino acid sufficiency. J Biol Chem. 2005; 280:23433–6. [PubMed: 15878852]
18. Brugarolas J, Lei K, Hurley RL, et al. Regulation of mTOR function in response to hypoxia by REDD1 and the TSC1/TSC2 tumor suppressor complex. Genes Dev. 2004; 18:2893–904. [PubMed: 15545625]
19. Sofer A, Lei K, Johannessen CM, Ellisen LW. Regulation of mTOR and cell growth in response to energy stress by REDD1. Mol Cell Biol. 2005; 25:5834–45. [PubMed: 15988001]
20. Thomas GV, Tran C, Mellinghoff IK, et al. Hypoxia-inducible factor determines sensitivity to inhibitors of mTOR in kidney cancer. Nat Med. 2006; 12:122–7. [PubMed: 16341243]
21. Sarkaria JN, Yang L, Grogan PT, et al. Identification of molecular characteristics correlated with glioblastoma sensitivity to EGFR kinase inhibition through use of an intracranial xenograft test panel. Mol Cancer Ther. 2007; 6:1167–74. [PubMed: 17363510]
22. Sarkaria JN, Carlson BL, Schroeder MA, et al. Use of an orthotopic xenograft model for assessing the effect of epidermal growth factor receptor amplification on glioblastoma radiation response. Clin Cancer Res. 2006; 12:2264–71. [PubMed: 16609043]
23. Whang YE, Wu X, Suzuki H, et al. Inactivation of the tumor suppressor PTEN/MMAC1 in advanced human prostate cancer through loss of expression. Proc Natl Acad Sci. 1998; 95:5246–50. [PubMed: 9560261]
24. Wei Q, Bondy ML, Mao L, et al. Reduced expression of mismatch repair genes measured by multiplex reverse transcription-polymerase chain reaction in human gliomas. Cancer Res. 1997; 57:1673–7. [PubMed: 9135006]
25. Eshleman J, Carlson B, Mladek A, Kastner B, Shide K, Sarkaria J. Inhibition of the mammalian target of rapamycin sensitizes U87 xenografts to fractionated radiation therapy. Cancer Res. 2002; 62:7291–7. [PubMed: 12499272]
26. Pandita A, Aldape KD, Zadeh G, Guha A, James CD. Contrasting *in vivo* and *in vitro* fates of glioblastoma cell subpopulations with amplified EGFR. Genes Chromosomes Cancer. 2003; 39:29–36. [PubMed: 14603439]
27. Galanis E, Buckner JC, Maurer MJ, et al. Phase II trial of temsirolimus (CCI-779) in recurrent glioblastoma multiforme: a North Central Cancer Treatment Group Study. J Clin Oncol. 2005; 23:5294–304. [PubMed: 15998902]
28. Chang SM, Wen P, Cloughesy T, et al. Phase II study of CCI-779 in patients with recurrent glioblastoma multiforme. Invest New Drugs. 2005; 23:357–61. [PubMed: 16012795]
29. Shinohara ET, Cao C, Niermann K, et al. Enhanced radiation damage of tumor vasculature by mTOR inhibitors. Oncogene. 2005; 24:5414–22. [PubMed: 15940265]
30. Lang SA, Gaumann A, Koehl GE, et al. Mammalian target of rapamycin is activated in human gastric cancer and serves as a target for therapy in an experimental model. Int J Cancer. 2007; 120:1803–10. [PubMed: 17230506]
31. Laschke MW, Elitzsch A, Scheuer C, Holstein JH, Vollmar B, Menger MD. Rapamycin induces regression of endometriotic lesions by inhibiting neovascularization and cell proliferation. Br J Pharmacol. 2006; 149:137–44. [PubMed: 16894343]
32. Guba M, von Breitenbuch P, Steinbauer M, et al. Rapamycin inhibits primary and metastatic tumor growth by antiangiogenesis: involvement of vascular endothelial growth factor. Nat Med. 2002; 8:128–35. [PubMed: 11821896]
33. Houchens DP, Ovejera AA, Riblet SM, Slagel DE. Human brain tumor xenografts in nude mice as a chemotherapy model. Eur J Cancer. 1983; 19:799–805.
34. Goudar RK, Shi Q, Hjelmeland MD, et al. Combination therapy of inhibitors of epidermal growth factor receptor/vascular endothelial growth factor receptor 2 (AEE788) and the mammalian target of rapamycin (RAD001) offers improved glioblastoma tumor growth inhibition. Mol Cancer Ther. 2005; 4:101–12. [PubMed: 15657358]
35. Heimberger AB, Wang E, McGary EC, et al. Mechanisms of action of rapamycin in gliomas. Neurooncol. 2005; 7:1–11.
36. Geoerger B, Kerr K, Tang C-B, et al. Antitumor activity of the rapamycin analog CCI-779 in human primitive neuroectodermal tumor/medulloblastoma models as single agent and in combination chemotherapy. Cancer Res. 2001; 61:1527–32. [PubMed: 11245461]

37. Faivre S, Kroemer G, Raymond E. Current development of mTOR inhibitors as anticancer agents. Nat Rev Drug Discov. 2006; 5:671–88. [PubMed: 16883305]

38. Choe G, Horvath S, Cloughesy TF, et al. Analysis of the phosphatidylinositol 3′-kinase signaling pathway in glioblastoma patients *in vivo*. Cancer Res. 2003; 63:2742–6. [PubMed: 12782577]

39. Jiang R, Mircean C, Shmulevich I, et al. Pathway alterations during glioma progression revealed by reverse phase protein lysate arrays. Proteomics. 2006; 6:2964–71. [PubMed: 16619307]

40. Riemenschneider MJ, Betensky RA, Pasedag SM, Louis DN. AKT activation in human glioblastomas enhances proliferation viaTSC2 and S6 kinase signaling. Cancer Res. 2006; 66:5618–23. [PubMed: 16740698]

41. Feng Z, Zhang H, Levine AJ, Jin S. The coordinate regulation of the p53 and mTOR pathways in cells. Proc Natl Acad Sci U S A. 2005; 102:8204–9. [PubMed: 15928081]

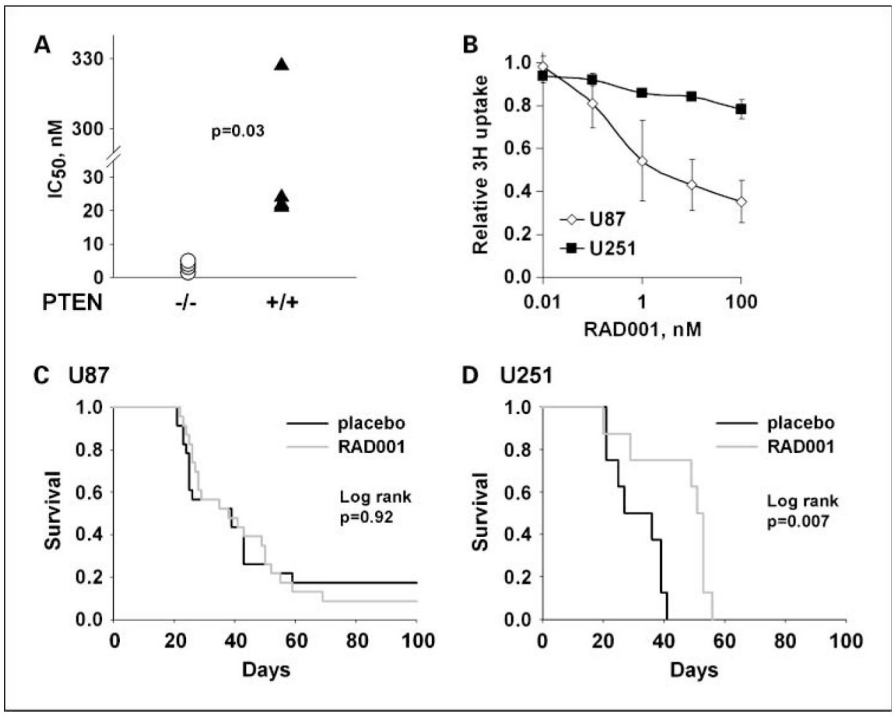


**Fig. 1.**

*In vitro* and *in vivo* RAD001 sensitivity in established gliomas tumor lines. *A,* $IC_{50}$ values for eight established tumor cell lines are plotted relative to their PTEN status (wild-type PTEN+/+, nonfunctional PTEN−/−). *B,* effects of RAD001 on [$^3$H]thymidine incorporation were evaluated following a 96-h incubation with drug in cell culture. Results of three independent experiments normalized to control treatment. Mean ± SE. Effects of RAD001 treatment on survival of orthotopic (*C*) U87 xenografts (pooled results from three experiments) or (*D*) U251 xenografts (single experiment).

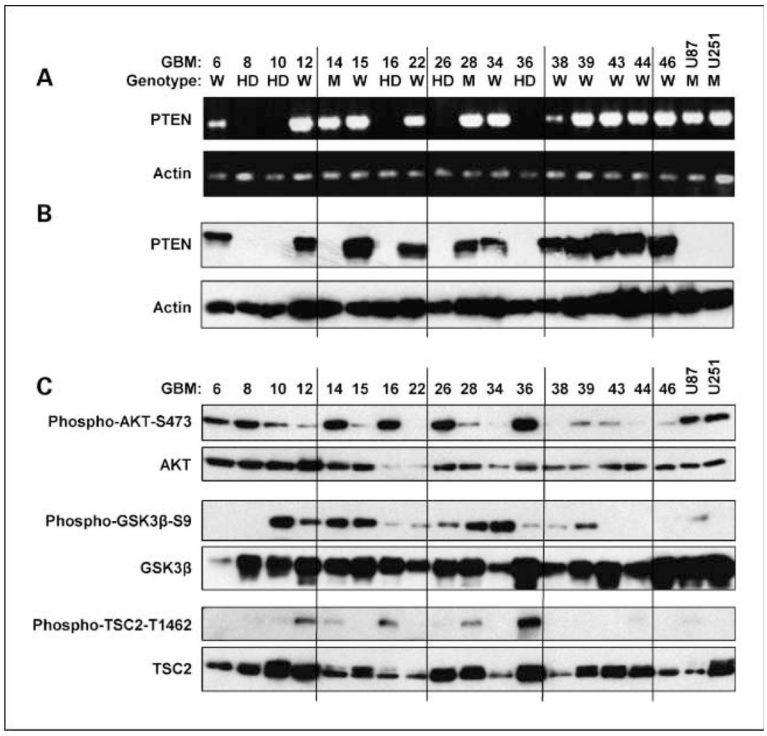


**Fig. 2.**

PTEN and Akt status in glioblastoma multiforme xenograft panel. Flank tumor specimens from each xenograft line were processed for analysis of the PI3K signaling pathway. *A*, reverse transcription-PCR using human-specific primers for PTEN. *Top*, results for the genomic analysis. *W*, wild-type; *M*, mutant; *HD*, homozygous deleted. *B*, Western blot analysis for PTEN expression and actin loading control. *C*, Western blot analysis from the same tumor specimens for the indicated phosphorylation sites and the corresponding total proteins.

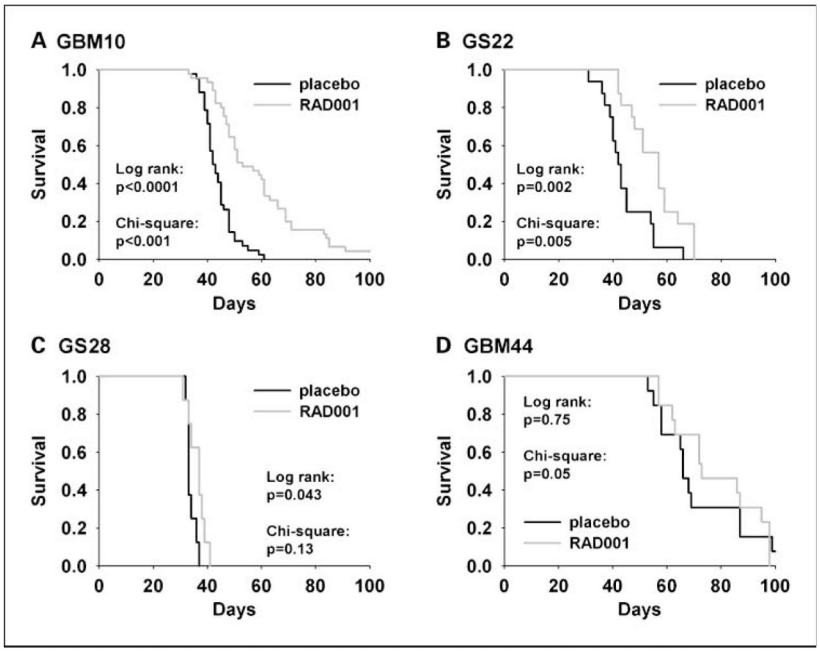


**Fig. 3.**

Survival following RAD001 treatment. Survival curves for mice with established intracranial tumors treated with vehicle control or RAD001. Results shown for GBM10 are pooled from six independent experiments, GS22 from two experiments, GS28 from one experiment, and GBM44 from two experiments.

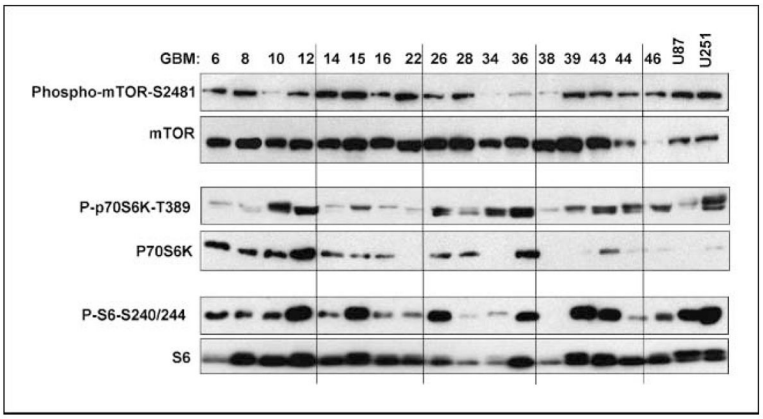


**Fig. 4.**

Western blot analysis of mTOR signaling. Flank tumor specimens were evaluated for activation of the mTOR signaling pathway by Western blotting with phosphorylation-specific and nonphosphorylation antibodies as indicated.

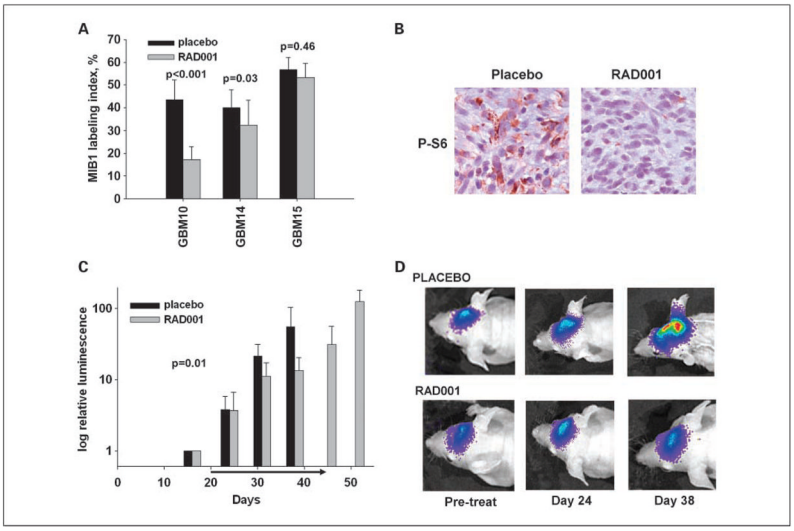


**Fig. 5.**

Effects of RAD001 treatment on intracranial tumors. Mice with established intracranial xenografts were randomized to therapy with RAD001 or placebo for 5 d before euthanasia and processing of tumor samples for immunohistochemistry. *A*, effects of treatment on MIB1 labeling. Mean ± SD for the indicated lines. *B*, immunohistochemistry for phospho-S6 in tumor sections from the resistant GBM15 tumor line treated with placebo or RAD001. *C*, GBM10 xenograft cells expressing firefly luciferase were used to establish intracranial tumors and then imaged serially starting on day16 after tumor implantation. Subsequent luminescence readings for each tumor were normalized to the day 16 readings. Mean ± SD for those mice that remain alive at any given time point. *Arrow*, interval of dosing from day 20 to day 45. *D*, serial bioluminescent images from a mouse treated with placebo or RAD001, respectively.

**Table 1**

RAD001 sensitivity

| Glioblastoma multiforme | PTEN | No. experiments | Placebo | | RAD001 | | Log-rank *P* | $\chi^2$ *P* | Δ Survival (%)* |
|---|---|---|---|---|---|---|---|---|---|
| | | | *n* | Median | *n* | Median | | | |
| GBM6 | WT | 3 | 21 | 63 | 21 | 75 | 0.13 | 0.35 | 19 |
| GBM8 | HD | 1 | 5 | 82 | 5 | 85 | 0.75 | 0.20 | 4 |
| GBM10 | HD | 6 | 42 | 42.5 | 45 | 53 | <0.0001 | <0.001 | 25 |
| GBM12 | WT | 2 | 16 | 28.5 | 16 | 31.5 | 0.66 | 0.48 | 11 |
| GBM14 | Mutant† | 3 | 25 | 42 | 25 | 43 | 0.46 | 0.78 | 2 |
| GBM15 | WT | 2 | 13 | 72 | 13 | 73 | 0.15 | 1.0 | 1 |
| GBM16 | HD | 1 | 8 | 47.5 | 8 | 61 | 0.92 | 0.32 | 28 |
| GS22 | WT | 2 | 16 | 42.5 | 16 | 57 | 0.002 | 0.005 | 34 |
| GBM26 | HD | 1 | 8 | 82.5 | 8 | 72 | 0.59 | 0.32 | −13 |
| GS28 | Mutant‡ | 1 | 8 | 33 | 8 | 37 | 0.043 | 0.13 | 12 |
| GBM34 | WT | 1 | 8 | 105 | 8 | 113.5 | 0.79 | 1.0 | 8 |
| GBM36 | HD | 1 | 5 | 67 | 5 | 62 | 0.42 | 0.53 | −7 |
| GBM38 | WT | 1 | 5 | 61 | 5 | 62 | 0.29 | 0.49 | 2 |
| GBM39 | WT | 1 | 8 | 87.5 | 6 | 101.5 | 0.23 | 0.28 | 16 |
| GBM43 | WT | 1 | 6 | 23.5 | 6 | 23.5 | 0.82 | 1.0 | 0 |
| GBM44 | WT | 2 | 13 | 66 | 13 | 73 | 0.75 | 0.050 | 11 |
| GBM46 | WT | 1 | 5 | 53 | 5 | 59 | 0.10 | 0.53 | 11 |

Abbreviations: WT, wild-type; HD, homozygous deleted.

*Relative change in median survival for RAD001-treated versus placebo-treated mice.

†2-bp deletion mutation in exon 1.

‡$Gly^{132}$ Asp missense mutation.